Nanoscale Research Letters

NANO EXPRESS Open Access

Biodegradation Assessment of Poly (Lactic Acid) Filled with Functionalized Titania Nanoparticles (PLA/TiO_2) under Compost Conditions

Yanbing Luo[1*], Zicong Lin[1] and Gang Guo[2*]

Abstract

This paper presents a biodegradation study conducted for 90 days under standardized controlled composting conditions of poly (lactic acid) (PLA) filled with functionalized anatase-titania nanofiller (PLA/TiO_2 nanocomposites). The surface morphology, thermal properties, percentage of biodegradation, and molecular weight changes at different incubation times were evaluated via visual inspection, scanning electron microscopy (SEM), X-ray diffraction (XRD), differential scanning calorimetry (DSC), and gel permeation chromatography (GPC) by taking degraded samples from compost at the end of target biodegradation time interval. The rapid increase of crystallinity indicated that the PLA and PLA/TiO_2 nanocomposites had heterogeneous degradation mechanisms under controlled composting conditions. The biodegradation rate of PLA/TiO_2 nanocomposites was higher than that of pure PLA because water molecules easily penetrated the nanocomposites. The dispersion of the nanoparticles in the PLA/TiO_2 nanocomposites affected the biodegradation rate of PLA. Moreover, the biodegradation of PLA could be controlled by adding an amount of dispersed TiO_2 nanofillers under controlled composting conditions.

Keywords: Biodegradation, PLA, Functionalized TiO_2, Compost

Introduction

Poly (lactic acid) (PLA), a synthetic biodegradable polymer, is investigated worldwide for biomedical and consumer applications because of the increasing need for renewable materials that are sustainable alternatives to petrochemical-derived products [1–4]. PLA is the product that results from the polymerization of lactide or lactic acid, which is the most extensively produced carboxylic acid in nature by microbial fermentation of carbohydrates [5]. However, the applicability of PLA has been relatively limited because its heat distortion temperature, toughness, and degradation rate are unsatisfactory [6, 7]. One of the methods to resolve these drawbacks is to modify PLA by adding inorganic nanoparticles, including typical nanoclay, carbon nanotubes, zinc oxide, and anatase (A-TiO_2) [8–15]. Recently, the PLA/TiO_2 nanocomposites were prepared by us via melting blending PLA with chemically modified TiO_2 (solution lactic acid grafted TiO_2, hereafter referred to as g-TiO_2) [16]. Results showed that TiO_2 nanoparticles had a significant effect on the improvement of the mechanical properties of the PLA/TiO_2 blends, such as strain at break and elasticity, compared with pure PLA. At the same time, g-TiO_2 nanoparticles had a strong influence on hydrolytic degradation and photodegradation of PLA [17, 18].

The study of biodegradability and biodegradation mechanism of biodegradable materials using laboratory-scale test is an extremely important method from industrial and scientific point of view which provides understanding of the service life of these materials [15]. There are several methods currently available to assess the biodegradability of biodegradable materials,

* Correspondence: luoybs@126.com; guogang@scu.edu.cn
[1]School of History and Culture, National Center for Experimental Archaeology Education, Sichuan University, Chengdu 610064, China
[2]State Key Laboratory of Biotherapy and Cancer Center, West China Hospital, West China Medical School, Sichuan University, Chengdu 610065, China

which are in general based on an indirect measurement, such as carbon dioxide production, biogas generation, or oxygen consumption [19, 20].

Biodegradation characteristics of PLA in compost have been studied and reported [21–23]. Composting is an accelerated biodegradation of organic materials in a warm, moist, and aerobic environment under a combination of microbial population and controlled composting conditions [24, 25]. Moreover, the biodegradation of PLA in composting conditions, a temperature- and humidity-dependent process, involves several processes, namely, water uptake, ester cleavage, and formation and dissolution of oligomer fragments [26]. The most accepted mechanism of the PLA biodegradation involves a two-step degradation process. Initially, the heat and moisture in the compost attack the PLA chains and split them apart, thereby producing small Mw polymers and, eventually, lactic acid. Thereafter, the microorganisms in the compost and soil mineralize the oligomer fragments and lactic acid to generate methane and carbon dioxide (CO_2) under anaerobic and aerobic conditions, respectively [27–29].

Recently, the effect of fillers on the biodegradation of PLA has attracted great attention and particular attention has been focused on nanofillers, such as nanoclays, carbon nanotubes, and hydroxyapatite [23, 30–38]. Some authors [32–34] found out that adding nanoparticles could accelerate biodegradation of PLA, which was attributed to the high relative hydrophilicity of the nanoparticles, thereby enabling the easy permeability of water into the polymer matrix and triggering hydrolytic degradation. However, other studies [35–38] reported that biodegradation was retarded because of the enhanced barrier properties of the nanocomposites.

Although there have been some literatures focusing on the biodegradation of PLA materials, the role that TiO_2 plays in PLA degradation remains controversial. How did the TiO_2 nanoparticles affect the biodegradation of PLA was not clear. So, a study of the biodegradation of PLA, modified by TiO_2 nanofillers under compost condition, is still needed. The current study, based on the estimation of the evolving CO_2, assessed the biodegradation of PLA/TiO_2 nanocomposites extensively under controlled laboratory compost conditions, a complement of degradability of the PLA/TiO_2 nanocomposites under different degradation conditions, could extend PLA's use in various end-use applications in the future.

Methods

Materials

PLA (manufactured by Natureworks@ (4032D)) exhibited a weight-average molecular weight (Mw) of 19,600 kDa and polydispersity of 1.89 as determined through gel permeation chromatography (GPC). PLA dried at 65 °C for 24 h under reduced pressure and stored in vacuum with humidity absorber before use. Lactic acid (88%, Guangshui National Chemical Co.) was distilled at 80 °C to remove water before use. The anatase titania nanoparticles, with an average primary particle size of ca. 20 nm, were supplied by Pangang Co., Ltd. Toluene and chloroform were used as received. Chromatographic grade microcrystalline cellulose was supplied by Shanghai Chemical Reagent Co., Ltd. The composting inoculums, which were obtained from an organic fraction of municipal solid waste (MSW), were supplied by the Degradable Plastics Professional Committee of the China Plastics Processing Industry Association (CPPIA).

Sample Preparation

Detailed information on the functionalization of the TiO_2 nanoparticles and preparation of the PLA/TiO_2 nanocomposites has been reported [16]. G-TiO_2 nanofillers were prepared by grafting lactic acid oligomer onto anatase surface. PLA/TiO_2 nanocomposites were prepared by melt blending via a corotating twin-screw extruder. Pure PLA was subjected to same mixing treatment so as to have the same thermal history as nanocomposites. The samples with 0, 0.5, 1.0, 2.0, 5.0, 8.0, and 15.0 wt% g-TiO_2 were prepared and labeled as PLA, PLA/TiO_2–0.5, PLA/TiO_2–1, PLA/TiO_2–2, PLA/TiO_2–5, PLA/TiO_2–8, and PLA/TiO_2–15 nanocomposites.

Small chip specimens of PLA and g-TiO_2 at different ratios were converted into sheets of approximately 0.5 mm in thickness by pressing at 190 °C for 4 min under 10 MPa followed by cooling at room temperature for 5 min under 5 MPa. Thereafter, the compression molded samples were cut into 5 mm × 5 mm size and weighed.

Degradation Tests

A biodegradation test was conducted in a laboratory scale-installation based on standard test methods designed for biodegradable plastics (GB/T19277–2003/ISO 14855-1:2005) (determination of the ultimate aerobic biodegradability of plastic materials under controlled composting conditions—method by analysis of evolved CO_2). Most of the carbon in the metabolized substrates generates energy through chemical transformation to CO_2 in aerobic environments [39]. Therefore, measurements of the generation of CO_2 are considered the most appropriate measure of biodegradation in most circumstances. The standard specifies a procedure to determine the ultimate aerobic biodegradability by measuring the amount of evolved CO_2 and percentage of the biodegradation degree of the test materials under controlled composting conditions. The composting inoculum was obtained from an organic fraction of MSW, which was sieved to sizes under 5 mm. Thereafter, the fine fraction was used as inoculums. Table 1 shows the determined

Table 1 Physicochemical properties of inoculums

Properties	Value	Test method
pH	7.2	GB/T 19277–2003 ISO 14855-2005
Total dry solid (TS) %	71.3	
Volatile solids (VS, % on TS)	19.3	
Residual ash content (RAC, % on TS)	80.7	
Moisture[a] (%)	53.5	
C/N ratio	15	

[a]Percentages are expressed on a dry weight loss

physicochemical properties of the composting inoculums. In each test, a series of composting reactors (each sample in triplicates) was loaded with 15 g of the reference material (i.e., microcrystalline cellulose (MCE), which was suggested by the standard) or test material (each film weighted and labeled before degradation), 85 g of inoculum, and 320 g of dry sea sand (provides good homogeneous conditions and an improved aerobic environment inside the inoculum). Thereafter, the reactors were placed in an incubator without light at 58 ± 2 °C through an experiment time of 90 days. Aeration was initiated using water-saturated CO_2-free air; the flow rate through each reactor was set at 25 mL·min^{-1}. The humidity, mixing, and aeration in all the reactors were controlled as established by the GB/T19277–2003/ISO 14855-12,005 requirements. At selected times, three to four specimens of each sample were selected, washed with distilled water, and dried at room temperature at least 24 h to constant weight.

The CO_2 that evolved during the biodegradation process was trapped in NaOH solutions and measured at regular intervals using titration method. The NaOH was titrated with standard HCl solution to the phenolphthalein endpoint. The total CO_2 evolved during biodegradation was calculated with reference to the control flask. The data reported for each sample was the mean value obtained from three samples.

Characterization

Microscope Examination

Scanning electron microscopy (SEM) images were obtained using a Philips FEI INSPECT F instrument operated at 5 kV. All specimens were sputter coated with gold prior to analysis.

Thermal Analysis

Thermal properties of samples were studied by differential scanning calorimetry (DSC) (TA Q20, TA Instruments). Thermograms were obtained under nitrogen flow (50 mL/min) at a heating and cooling rates of 10 °C/min in the temperature range from room temperature to 200 °C and from 200 to − 50 °C, respectively.

XRD Studies

X-ray diffraction (XRD) analyses were performed using a DX-1000 X-ray diffractometer (Dandong Fanyuan Instrument Co. LTD. China) equipped with a Cu K_α (λ = 0.154 nm) source. The generator was operated at 25 mA and 40 kV. Samples were scanned at different angles (i.e., from 2 to 70°) at a scanning rate of 6°/min.

Determination of the Percent of Biodegradation (D_t, %)

Percent of biodegradation (D_t, %) could be calculated using Eq. 1, which was adopted as for Eq. 2 [1, 40].

$$D_t(\%) = \frac{(CO_2)_T - (CO_2)_B}{Th_{CO2}} \times 100 \quad (1)$$

where $(CO_2)_T$ is the amount of CO_2 (in g/flask) evolved from the test materials, $(CO_2)_B$ is the amount of CO_2 (in g/flask) evolved in the control flask, and Th_{CO2} is the theoretical CO_2 amount produced by the polymeric materials.

The theoretical CO_2 amount that can be produced in each flask (Th_{CO2}, g^2/g sample) was calculated using the following equation:

$$Th_{CO2} = M_{TOT} \times C_{TOT} \times \frac{44}{12} \quad (2)$$

where M_{TOT} is the total weight (g) of the dry polymeric solids material added into the composting flask at the start of the experiment, C_{TOT} is the weight (g) of the total organic carbon in the total dry polymeric solids in the sample, and 44 and 12 are the molecular mass of CO_2 and atomic mass of C, respectively.

Molecular Weight Measurement

The molecular weights of the PLA nanocomposites before and after composting were determined through GPC. The GPC system was equipped with a Waters 1515 Isocratic HPLC pump, a Waters 2414 refractive index detector, and Waters 717 plus autosampler. Chloroform was used as eluent at 0.8 mL/min flow rate at 30 °C. Calibration was accomplished with polystyrene standards.

Results and Discussion

Polymer degradation is associated with changes in characteristics, such as color, surface morphology, and mechanical properties. The temporal changes in the appearance of the pure PLA and PLA/TiO_2 nanocomposites were different under laboratory conditions. The pure PLA matrix surfaces, which were initially transparent in agreement with the amorphous structure, became relatively whitish after 2 days of biodegradation [41]. This feature increased with incubation time until complete opacity after 10 days. Yellowy to dark brown

plaques, caused by water permeation and microorganisms incubation, began to be observed on the surface of neat PLA films surface after 30 days. However, large area of dark brown plaques emerged on the surface of PLA nanocomposite after 6 days (figure was not shown). The brown spots imply the microorganism colonies and the cracks represent the biodegradation effect. Figure 1 shows the surface morphology of PLA and its TiO_2 nanocomposites under SEM observation. Before degradation, the surface of neat and PLA/TiO_2 nanocomposites were smooth. Neat PLA did not present significant changes on the surface after biodegradation 5 days in compost conditions. After 20 days, the surface roughness of neat PLA increased (Fig. 1a, a'). However, PLA/TiO_2 nanocomposite exhibited progressive changes clearly showing that considerable degradation of PLA/TiO_2 composite occurred. Obvious cracks and voids (Fig. 1b, b'; c, c'; and d, d'; respectively) were observed on the surface of nanocomposites. This could be owned to the hydrolysis of PLA and microorganisms activities. With increasing incubation time, the cracks and voids became substantially deep and large (Fig. 1 b', c', and d', respectively), thereby suggesting chain loss and surface erosion as time progresses. The bulk erosion phenomenon for all test materials was similar to the hydrolytic degradation process of the PLA and PLA/TiO_2 nanocomposites [17].

To evaluate the crystallinity of the PLA and PLA/TiO_2 nanocomposites during biodegradation, samples selected at different incubation times were analyzed for their thermal properties (Figs. 2 and 3). Figure 2 shows that the glass transition temperature (T_g) decreased slightly for all samples with degradation time. The decrease of T_g was clearly due to an enhanced mobility of the molecules, as a consequence of the hydrolysis process and plasticizing effect of the oligomer fragments and water during biodegradation [33, 42]. The disappearance of cold crystallization peak (T_{cc}) for all of the samples only after 2 days could be ascribed to the hydrolysis of PLA and the rapid increase in crystallinity of the polymer matrix [43]. The decrease of T_m was ascribed to the rapid molecular mass reduction [44, 45]. The bimodal melting peak gradually changed to monomodal peak, thereby implying that the small and imperfect crystals disappeared with degradation time. This result proved that the degradation of PLA proceeded rapidly in the amorphous regions during the early stage of degradation under controlled composting conditions. The cooling scan (see Fig. 3) shows that the crystallization peak of the neat PLA increased gradually. However, the crystallization peaks of the PLA/TiO_2 nanocomposites initially increased significantly and decreased slightly thereafter with an increase in incubation time. Moreover, the higher the nanofillers content was, the earlier the crystallization peaks arrived at its peak. The decrease of crystallization peak further verified that the crystalline region began to degrade after the degradation of the amorphous region. Giuliana and Roberto [42] reported that at short times for PLA sample some amorphous regions change into crystal, then the crystallinity degree increases due to the effect of the erosion of the amorphous parts. Moreover, the crystalline regions undergo hydrolysis at long times.

XRD provides an ideal method to monitor changes in the crystallization of polymers during degradation. The XRD patterns of PLA and its nanocomposites (Fig. 4) show that the polymer matrix maintains an amorphous structure before biodegradation. Only after 2 days, two strong peaks at $2\theta = 16.4$, 18.5°, 20.9°, and 23.6° clearly appeared and their intensity increased with incubation time. This result implied that poly (L-lactide) or poly (D-lactide)-type crystalline structures were formed [46, 47]. The change of crystalline peak indicated that amorphous regions degraded more rapidly than crystalline regions, which increased the crystalline-to-amorphous regions ratio value. This result was consistent with DSC results and the transparency change of the samples.

The evaluation of the inoculum validation is crucial during biodegradation under composting conditions. The activity of the inoculum was measured as required by the standard method: D_t of the reference material should be at least 70% at the end of the 45 days of testing. The insert in Fig. 5 shows that MCE begins to biodegrade after 5 days, and the percentage of biodegradation is up to 72% at the end of the 45 days of incubation. These result indicated that MCE in the experiment was effective as a reference material. In the experiment, duplicate composting vessels showed good reproducibility (standard deviation ± 1.3%). Figure 5 shows D_t for neat PLA and PLA/TiO_2 nanocomposites during incubation. A similar behavior was observed for the PLA and PLA/TiO_2 nanocomposites, that is, a lag phase was first observed which is then followed by a steep linear increase in biodegradation and thereafter by a plateau phase for all samples. The steepness of the increase should be indicative of increased degradation. However, the curves indicated that the lag phase of the nanocomposites was a little shorter than that of pure PLA. This result indicated the presence of TiO_2, at some degree, accelerated the initial phase of degradation and increased the percentage of CO_2 produced at the end of the incubation period. After 80 days of incubation under controlled composting conditions, D_t for PLA, PLA/TiO_2–1, PLA/TiO_2–2, PLA/TiO_2–5, PLA/TiO_2–8, and PLA/TiO_2–15 reached up to 78.9, 86.9, 92.0, 97.8, 91.3, and 85.0%, respectively. Kunioka et al. [48] reported that the final biodegradability of PLA was 80%. The results

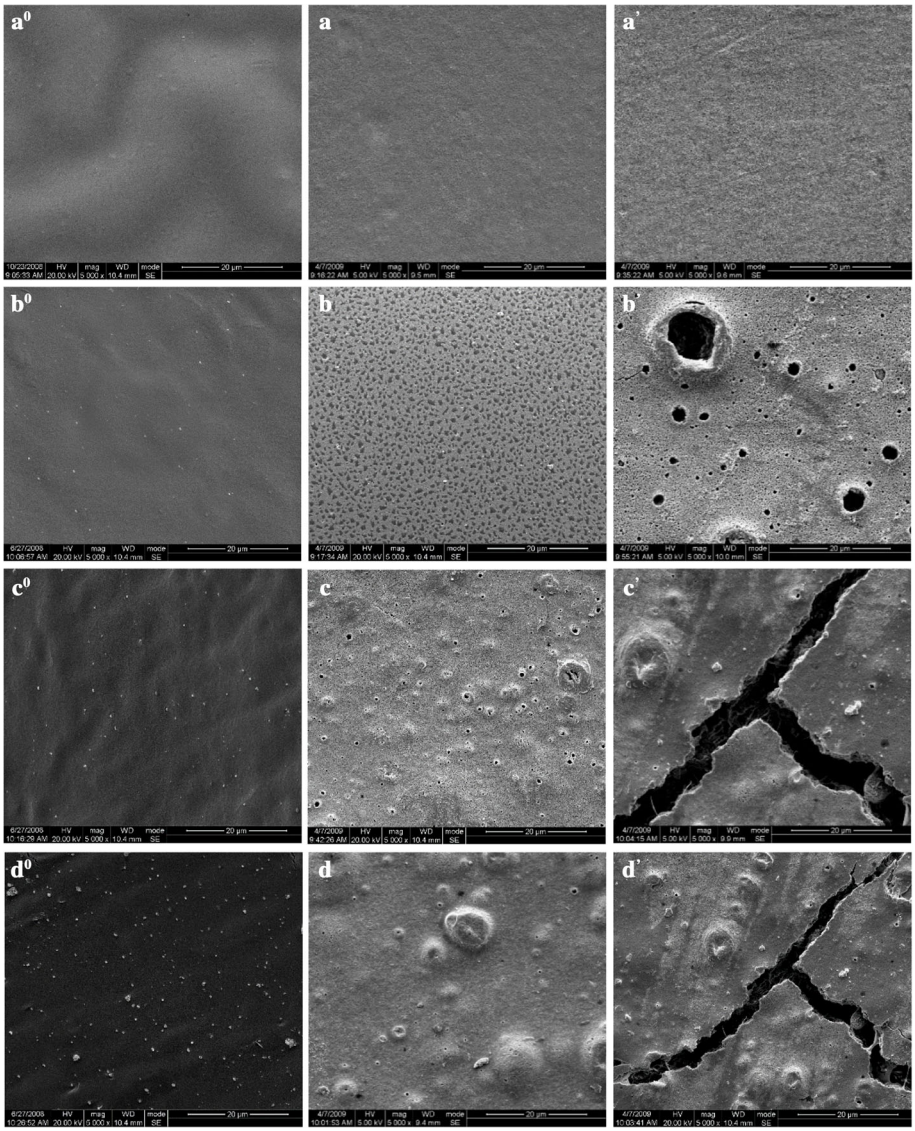

Fig. 1 SEM photography of the surface of pure PLA (**a⁰**, **a**, **a′**), PLA/TiO_2–2 (**b⁰**, **b**, **b′**), PLA/TiO_2–5 (**c⁰**, **c**, **c′**) and PLA/TiO_2–8 (**d⁰**, **d**, **d′**) nanocomposites as a function of incubation time. **a⁰**, **b⁰**, **c⁰**, **d⁰**:0 day; **a**, **b**, **c**, **d**: 5 days; **a′**, **b′**, **c′**, **d′**: 20 days

from our experiment showed that D_t of the commercially pure PLA product was also nearly 80% at the end of 80 days. The decrease of D_t beginning from PLA/TiO_2–8 is ascribed to the intense agglomeration of TiO_2 when its content was beyond 8 wt% [16]. Further details are presented in the following section.

The different percentages of biodegradation are related to the different molecular weight changes of the polymer matrix. Figure 6 shows the molecular weight change of the samples as a function of incubation time. The curves show that the changes of Mn in the PLA/TiO_2 nanocomposites were similar (i.e., a rapid decrease of Mn followed by a plateau phase of nearly a constant Mn) at least in the determined incubation time. To explore the degradation mechanisms caused by the addition of nanofillers, a model that accounts for autocatalysis by the generated carboxylic acid end groups was used to calculate the catalyzed degradation rate constant according to reference [17, 49]:

$$\ln M_{nt} = \ln M_{n0} - kt \tag{3}$$

where k is catalyzed hydrolytic degradation rate constant, M_{n0} is the number-average molecular weight before degradation, M_{nt} is the number-average molecular weight at any time.

The k values evaluated by Eq. (3) are plotted in Fig. 7. From Fig. 7, the degradation rate of the PLA and PLA nanocomposites could be identified to two and three phases, respectively. Mn decreased rapidly during the

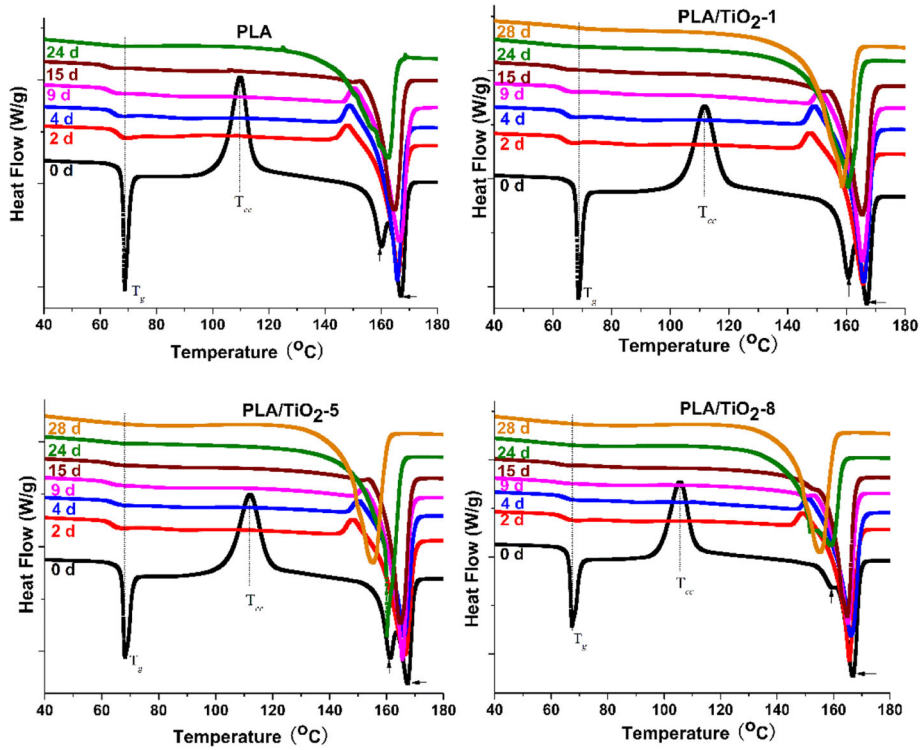

Fig. 2 DSC thermograms of biodegradation products of pure PLA and PLA/TiO_2 nanocomposites at different incubation times, first heating scan

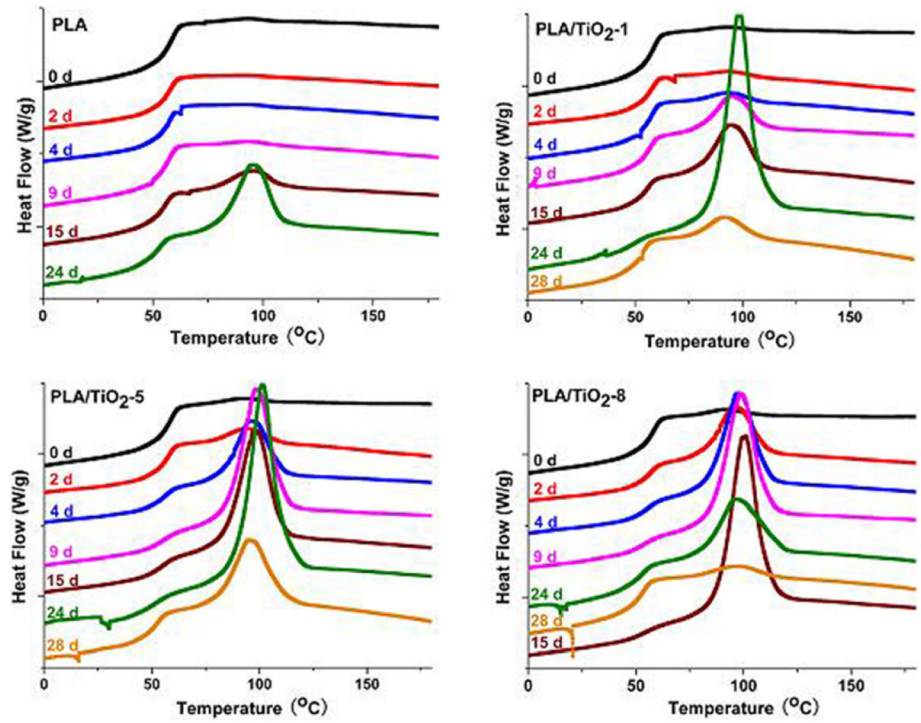

Fig. 3 DSC thermograms of biodegraded pure PLA and PLA/TiO_2 nanocomposites at different incubation times, cooling scan

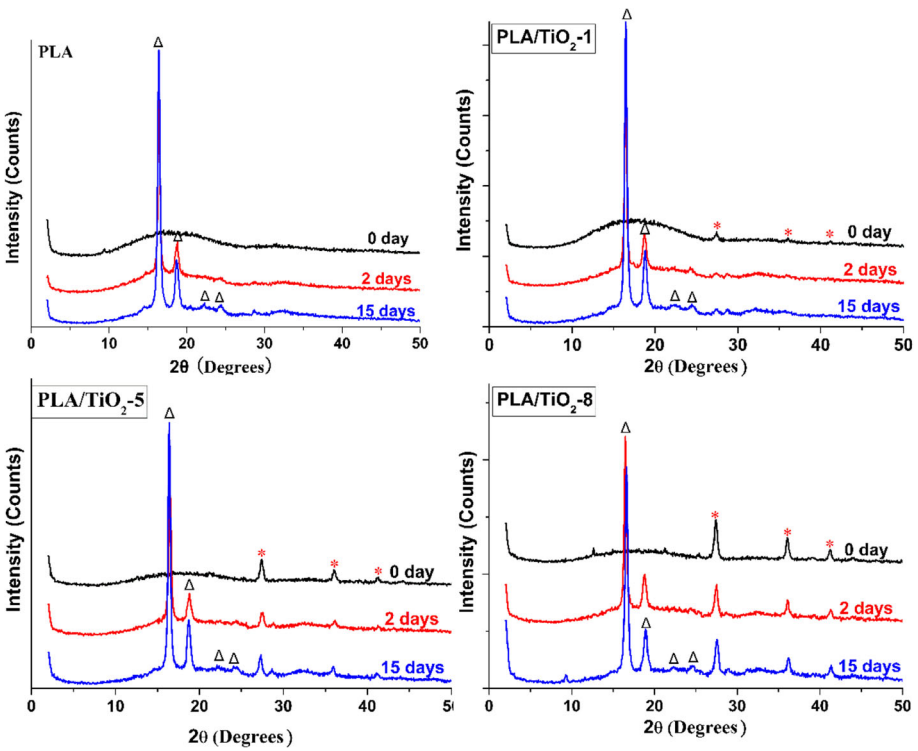

Fig. 4 XRD patterns of pure PLA and PLA/TiO_2 nanocomposites at different incubation times

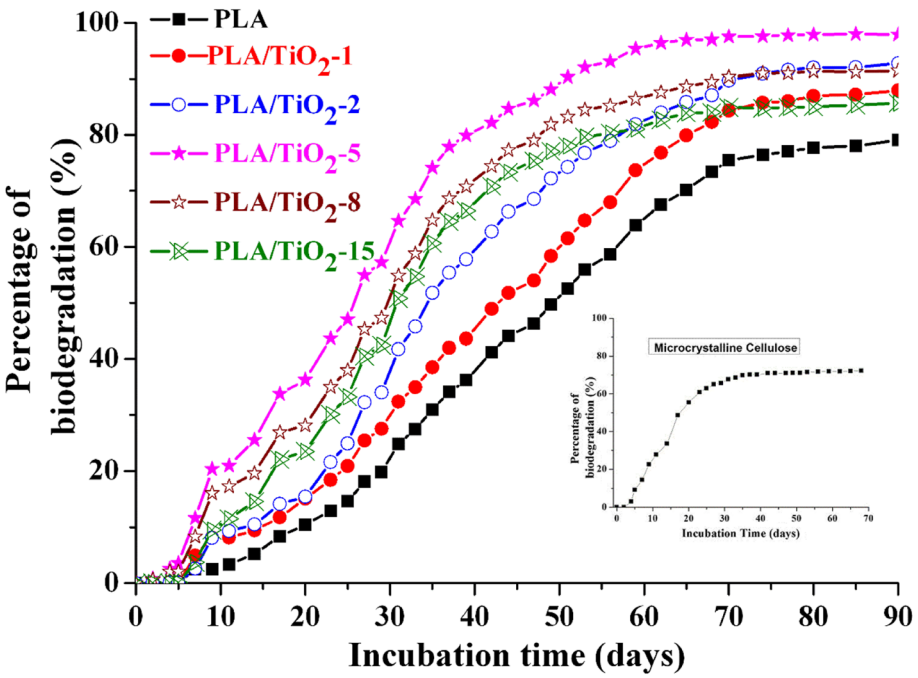

Fig. 5 Percentage of biodegradation as a function of incubation time for pure PLA and PLA/TiO_2 nanocomposites. The insert is the percentage of biodegradation as a function of time for microcrystalline cellulose

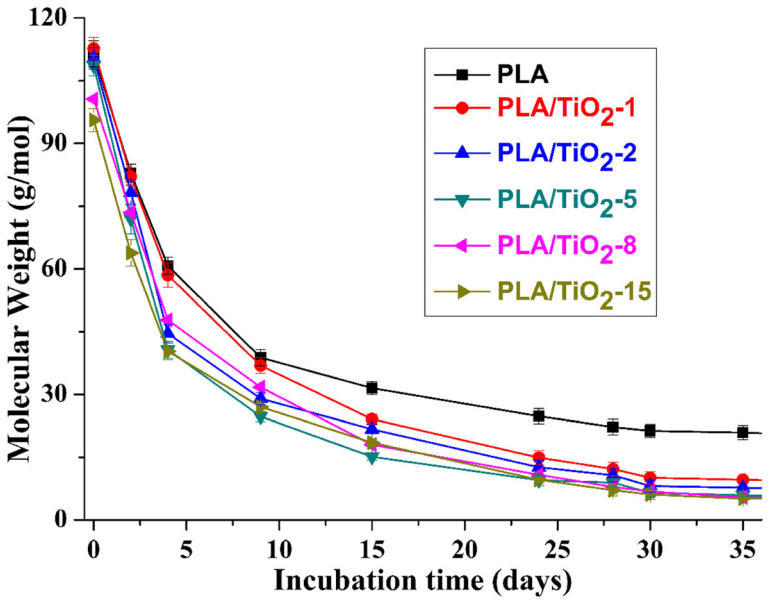

Fig. 6 Change of Mn as a function of time for pure PLA and PLA/TiO_2 nanocomposites

first 8 days and followed by a plateau phase thereafter for neat PLA. For PLA/TiO_2 nanocomposites, the highest values of k means that M_n decreased rapidly in the first phase (i.e., from 0 to 4 days). The following 5 to 24 days are ascribed to the second phase, and the values of k decreased slightly compared with the first phase. Few studies [13, 50] showed that the crystalline part of PLA was more resistant to degradation than the amorphous part; thus, the decrease in k in this phase could be caused by the increase of crystallinity of the PLA matrix. After 24 days (i.e., the last phase), the value of k decreased again. At this stage, the polymer completely degraded into oligomer fragments or lactic acid, and the microorganisms mineralized the remaining materials to continuously generate CO_2.

Under composting conditions, the factors that affect the biodegradation tendency of PLA would control the degradation of the PLA/TiO_2 nanocomposites. When an amount of g-TiO_2 was homogeneously dispersed in the PLA matrix, the water molecules penetrated easily within the samples to trigger the degradation process [17]. Consequently, Mn decreased substantially in the

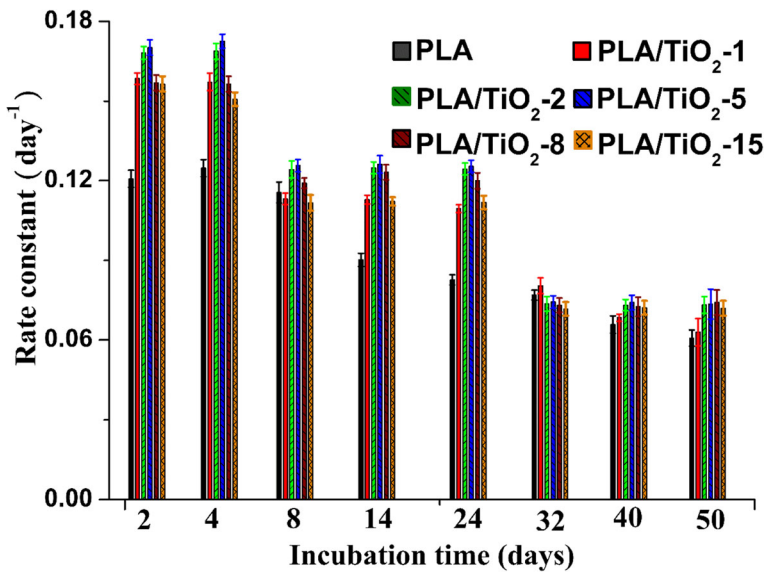

Fig. 7 Biodegradation rate versus incubation time for pure PLA and PLA/TiO_2 nanocomposites

first phase. The evolution of the lag phase of CO_2 for PLA and its nanocomposites during this period indicated that microorganisms need suitable polymer chains to mineralize. With increased incubation time, the polymer chains in amorphous regions degraded and the number of amorphous regions decreased; thus, the percentage of crystalline to the amorphous region (i.e., χ_c) increased [39], thereby leading to the decrease of k in the second phase. However, the oligomer fragments began to be mineralized by microorganisms in this stage, thereby indicating that the productive phase for the PLA mineralization occurred. With the decrease of the remaining oligomer fragments and the increase of χ_c, k and D_t decreased and a nearly long plateau phase was observed for k and D_t in the third stage. In our previous study [16], the morphology of each nanocomposite was reported and determined through SEM and TEM; the results showed that the dispersion of g-TiO_2 with under 5 wt% in the PLA/TiO_2 nanocomposites was better than that obtained with a high concentration of nanofillers. In terms of the dispersion and content of TiO_2, PLA/TiO_2–5 had the largest k and D_t compared with the other nanocomposites in our experiment.

Conclusions

PLA/TiO_2 nanocomposites were prepared (based on PLA and functionalized g-TiO_2) and subjected to biodegradation under controlled composting conditions. Using such a standard, the information of patterns on the surface of the samples and the rapid increase of crystallinity indicated that the PLA and PLA/TiO_2 nanocomposites had heterogeneous biodegradation mechanisms. The degradation study of nanocomposites under composting conditions showed that the inherent degradable character of PLA remained after the incorporation of functionalized titania nanoparticles (PLA/TiO_2). The addition of the TiO_2 nanoparticles increased the degradation rate of the PLA matrix because the water molecules easily penetrated the PLA/TiO_2 nanocomposites, thereby activating the degradation process. This phenomenon was particularly evident for PLA/TiO_2–5 because of its high TiO_2 content and good dispersion of TiO_2 nanofillers in the PLA matrix compared with other nanocomposites.

Abbreviations

DSC: Differential scanning calorimetry; D_t: Percent of biodegradation; GPC: Gel permeation chromatography; g-TiO_2: Grafted TiO_2; MCE: Microcrystalline cellulose; Mn: Number-average molecular weight; Mw: Weight-average molecular weight; PLA: Poly (lactic acid); SEM: Scanning electron microscopy; T_{cc}: Cold crystallization peak; T_g: Glass transition temperature; XRD: X-ray diffraction

Acknowledgements

This work was supported by the Key projects of social science planning in Sichuan Province SC18A013 and Sichuan University Research Cluster for Regional History and Frontier Studies.

Funding

The authors gratefully acknowledge the financial support from High Level Research Team Building Plan of Social Sciences in Sichuan Province (Sichuan Federation of Social Science Association [2017] 43–2) and Advanced Interdisciplinary Innovation Research Project of Sichuan University (skqy201216).

Availability of data and materials

All the data are fully available without restriction.

Authors' contributions

LYB contributed to the experimental work, data analysis, and was a major contributor in writing the manuscript. LZC contributed to the experimental work and data analysis. GG analyzed and interpreted the data. All authors read and approved the final manuscript.

Competing interests

The authors declare that they have no competing interests.

Publisher's Note

Received: 15 October 2018 Accepted: 4 February 2019
Published online: 14 February 2019

References

1. Castro-Aguirre E, Iñiguez-Franco F, Samsudin H, Fang X, Auras R (2016) Poly (lactic acid)—mass production, processing, industrial applications, and end of life. Adv Drug Deliv Rev 107:333–366
2. Cadar O, Paul M, Roman C, Miclean M, Majdik C (2012) Biodegradation behavior of poly (lactic acid) and (lactic acid-ethylene glycol-malonic or succinic acid) copolymers under controlled composting conditions in a laboratory test system. Polym Degrad and Stab 97(3):354–357
3. Deroiné M, Le Duigou A, Corre YM, Le Gac PY, Davies P, César G, Bruzaud S (2014) Accelerated ageing of polylactide in aqueous environments: comparative study between distilled water and seawater. Polym Degrad Stab 108:319–329
4. Pantani R, Sorrentino A (2013) Influence of crystallinity on the biodegradation rate of injection-moulded poly (lactic acid) samples in controlled composting conditions. Polym Degrad Stab 98:1089–1096
5. Murariu M, Dubois P (2016) PLA composites: from production to properties. Adv Drug Deliv Rev 107:17–46
6. Sinha RP, Pandey JK, Rutot D, Degeé P, Dubois P (2003) Biodegradation of poly (3-caprolactone)/starch blends and composites in composting and culture environment: the effect of compatibilization on the inherent biodegradability of the host polymer. Carbohydr Res 338(17):1759–1769
7. Zhou YH, Lei L, Yang B, Li JB, Ren J (2018) Preparation and characterization of polylactic acid (PLA) carbon nanotube nanocomposites. Polym Test 68: 34–38
8. Cele HM, Ojijo V, Chen H, Kumar S, Land K, Joubert T, de Villiers MFR, Ray SS (2014) Effect of nanoclay on optical properties of PLA/clay composite films. Polym Test 36:24–31
9. Hakim RH, Cailloux J, Santana OO, Bou J, Sábchez-Soto M, Odent J, Raquez JM, Dubios P, Carrasco F, Maspoch MLI (2017) PLA/SiO_2 composites: influence of the filler modifications on the morphology, crystallization behavior, and mechanical properties. J Appl Polym Sci 134. https://doi.org/10.1002/app.45367
10. Costa RGF, Brichi GS, Ribeiro C, Mattoso LHC (2016) Nanocomposite fibers of poly (lactic acid)/titanium dioxide prepared by solution blow spinning. Polym Bull 73(11):1–13
11. Wu JH, Kuo MC, Chen CW (2015) Physical properties and crystallization behavior of poly (lactide)/poly (methyl methacrylate)/silica composites. J Appl Polym Sci 132. https://doi.org/10.1002/app.42378
12. Ramos M, Fortunati E, Peltzer M, Jimenez A, Kenny JM, Garrigós MC (2016) Characterization and disintegrability under composting conditions of PLA-based nanocomposite films with thymol and silver nanoparticles. Polym Degrad Stab 132:2–10
13. Raquez JM, Habibi Y, Murariu M, Dubois P (2013) Polylactide (PLA)-based nanocomposites. Prog Polym Sci 38(10):1504–1542

14. González A, Dasari A, Herrero B, Plancher E, Santarén J, Esteban A, Lim SH (2012) Fire retardancy behavior of PLA based nanocomposites. Polym Degrad Stab 97(3):248–256
15. Murariu M, Doumbia A, Bonnaud L, Dechief AL, Paint Y, Ferreira M, Campagne C, Devaux E, Dubois P (2011) High-performance polylactide/ZnO nanocomposites designed for films and fibers with special end-use properties. Biomacromolecules 12(5):1762–1771
16. Luo YB, Li WD, Wang XL, Xu DY, Wang YZ (2009) Preparation and properties of nanocomposites based on poly (lactic acid) and functionalized TiO_2. Acta Mater 57(11):3182–3191
17. Luo YB, Wang XL, Wang YZ (2012) Effect of TiO_2 nanoparticles on the long-term hydrolytic degradation behavior of PLA. Polym Degrad Stab 97:721–728
18. Luo YB, Cao YZ, Guo G (2018) Effects of TiO_2 nanoparticles on the photodegradation of poly (lactic acid). J Appl Polym Sci 135:1–8
19. Pagga U (1997) Testing biodegradability with standardized methods. Chemosphere 35(12):2953–2972
20. Massardier-Nageotte V, Pestre C, Cruard-Pradet T, Bayard R (2006) Aerobic and anaerobic biodegradability of polymer films and physico-chemical characterization. Polym Degrad Stab 91(3):620–627
21. Sedničková M, Pekařová S, Kucharczyk P, Bočkaj J, Janigová I (2018) Changes of physical properties of PLA-based blends during early stage of biodegradation in compost. Int J Biol Macromol 113:434–442
22. Ho KLG, Pometto AL, Gadea A, Briceño JA, Rojas A (1999) Degradation of polylactic acid (PLA) plastic in Costa Rican soil and Iowa state university compost rows. J Environ Polym Degrad 7(4):173–177
23. Tsuji H, Mizuno A, Ikada Y (1998) Blends of aliphatic polyesters. III. Biodegradation of solution-cast blends from poly (L-lactide) and poly (3-caprolactone). J Appl Polym Sci 70(11):2259–2268
24. Ghorpade VM, Gennadios A, Hanna MA (2001) Laboratory composting of extruded poly (lactic acid) sheets. Bioresour Technol 76(1):57–61
25. Nampoothiri KM, Nair NR, John RP (2010) An overview of the recent developments in polylactide (PLA) research. Bioresour Technol 101(22): 8493–8501
26. Göpferich A (1996) Mechanisms of polymer degradation and erosion. Biomaterials 17(2):103–114
27. Hakkarainen M (2002) Aliphatic polyesters: abiotic and biotic degradation and degradation products. Adv Polym Sci 157:113–138
28. Longieras A, Tanchette JB, Erre D, Braud C, Copinet A (2007) Compostability of poly (lactide): degradation in an inert solid medium. J Polym Environ 15(3):200–206
29. Saadi Z, Rasmont A, Cesar G, Bewa H, Benguigui L (2012) Fungal degradation of poly(l-lactide) in soil and in compost. J Polym Environ 20(2): 273–282
30. Castro-Aguirre E, Auras R, Selke S, Rubino M, Marsh T (2018) Enhancing the biodegradation rate of poly (lactic acid) films and pla bio-nanocomposites in simulated composting through bioaugmentation. Polym Degrad Stab 154:46–54
31. Brzezinski M, Biela T (2014) Polylactide nanocomposites with functionalized carbon nanotubes and their stereocomplexes: a focused review. Mater Lett 121:244–250
32. Lee SR, Park HM, Lim H, Kang T, Li X, Cho WJ et al (2002) Microstructure, tensile properties, and biodegradability of aliphatic polyester/clay nanocomposites. Polymer 43(8):2495–2500
33. Paul MA, Delcourt C, Alexandre M, Degée P, Monteverde F, Dubois P (2005) Polylactide/ montmorillonite nanocomposites: study of the hydrolytic degradation. Polym Degrad Stab 87(3):535–542
34. Fukushima K, Abbate C, Tabuani D, Gennari M, Camino G (2009) Biodegradation of poly (lactic acid) and its nanocomposites. Polym Degrad Stab 94(10):1646–1655
35. Someya Y, Kondo N, Shibata M (2007) Biodegradation of poly (butylene adipate-co-butylene terephthalate)/layered-silicate nanocomposites. J Appl Polym Sci 106(2):730–736
36. Wu TM, Wu CY (2006) Biodegradable poly (lactic acid)/chitosan-modified montmorillonite nanocomposites: preparation and characterization. Polym Degrad Stab 91(9):2198–2204
37. Wu KJ, Wu CS, Chang JS (2007) Biodegradability and mechanical properties of polycaprolactone composites encapsulating phosphate-solubilizing bacterium *Bacillus* sp. PG01. Process Biochem 42(4):669–675
38. Fukushima K, Abbate C, Tabuani D, Gennari M, Rizzarelli P, Camino G (2010) Biodegradation trend of poly(ε-caprolactone) and nanocomposites. Mater Sci Eng C 30(4):566–574
39. Selke S, Auras R, Nguyen TA, Aguirre EC, Cheruvathur R, Liu Y (2015) Evaluation of biodegradation-promoting additives for plastics. Environ Sci Technol 49:3769–3777
40. Kim MC, Masuoda T (2009) Degradation properties of PLA and PHBV films treated with CO_2-plasma. React Funct Polym 69(5):287–292
41. Lv SS, Zhang YH, Gu JY, Tan HY (2018) Physicochemical evolutions of starch/poly (lactic acid) composite biodegraded in real soil. J Environ Manag 228:223–231
42. Giuliana G, Roberto P (2013) Effect of PLA grades and morphologies on hydrolytic degradation at composting temperature: assessment of structural modification and kinetic parameters. Polym Degrad Stab 98(5):1006–1014
43. Ebadi-Dehaghani H, Barikani M, Borhani S, Bolvardi B, Khonakdar HA, Jafari SH (2016) Biodegradation and hydrolysis studies on polypropylene/ polylactide/organo-clay nanocomposites. Polym Bull 73(12):3287–3304
44. Ratto JA, Stenhouse PJ, Auerbach M, Mitchell J, Farrell R (1999) Processing, performance and biodegradability of a thermoplastic aliphatic polyester/ starch system. Polymer 40(24):6777–6788
45. Hakkarainen M, Karlsson S, Albertsson AC (2000) Rapid (bio) degradation of polylactide by mixed culture of compost microorganisms-low molecular weight products and matrix changes. Polymer 41(7):2331–2338
46. Li S, McCarthy S (1999) Further investigations on the hydrolytic degradation of poly (DL-lactide). Biomaterials 20(1):35–44
47. von Recum HA, Cleek RL, Eskin SG, Mikos AG (1995) Degradation of polydispersed poly (L-lactic acid) to modulate lactic acid release. Biomaterials 16(6):441–447
48. Kunioka M, Ninomiya F, Funabashi M (2006) Biodegradation of poly (lactic acid) powders proposed as the reference test materials for the international standard of biodegradation evaluation methods. Polym Degrad Stab 91(9): 1919–1928
49. Biodegradation of poly (lactic acid) powders proposed as the reference test materials for the international standard of biodegradation evaluation methods (2006) Polym Degrad Stab 91(9):1919–1928
50. Tsuji H, Ikada Y (2000) Properties and morphology of poly (L-lactide) 4. Effects of structural parameters on long-term hydrolysis of poly (L-lactide) in phosphate-buffered solution. Polym Degrad Stab 67(1):179–189